CHAPTER SEVEN

7. MODEL DEVELOPMENT: SOIL MOISTURE MODEL ABDOMEN

To apply the soil moisture profile estimation algorithm established in Chapter 6 to a catchment scale field application, a catchment scale soil moisture profile forecasting model was required. In Chapter 5, the necessity for modelling soil temperature in addition to soil moisture was highlighted. However, unlike soil moisture, soil temperature could only be monitored for one soil profile in the Nerrigundah catchment, meaning that the soil temperature estimation could not be evaluated in this thesis. Hence, the forecasting model for the field application was only required to forecast the spatial distribution of soil moisture profiles. This chapter develops a computationally efficient soil moisture profile forecasting model for application to both one-dimensional (Chapter 10) and three-dimensional
(Chapter 11) field applications of the soil moisture profile estimation algorithm. using the data collected for the Nerrigundah experimental catchment (Chapter 9).

7.1 MODEL REQUIREMENTS

The requirements for the catchment scale soil moisture profile model, such that it can be used with the Kalman-filter assimilation scheme, are:

i) Be of a form such that the soil moisture state equations can be expressed, using linear algebra, as an explicit function of the soil moisture states at the previous time step.

ii) Describe the spatial distribution and temporal variation of soil moisture profiles, and not just profile storage.

iii) Have a thin near-surface layer that is compatible with the soil moisture observation depth.

iv) Have a spatial discretisation that is compatible with the spatially distributed near-surface soil moisture observations (ie. grid based).

v) Be relatively simple, requiring a minimal amount of computational effort.

vi) Allow for both capillary rise during drying events and gravity drainage during wetting events.

vii) Allow for lateral redistribution.

viii) Require no assumption about a water table at some depth.

ix) Be in a form that will allow correlations to build up between soil layers and grid elements.

x) Be in as linear form as possible (ie. model volumetric soil moisture content as the dependent state).

The importance of (ix) is in the updating of soil moisture content for deeper depths in the soil profile. Using the Kalman-filter assimilation scheme, this only occurs if the forecast covariance matrix of system states suggests there is a correlation with the near-surface soil moisture observations. Likewise, if observations are made for only a portion of the catchment, horizontal correlations allow updating of grid elements where observations are unavailable. These correlations are generated if the change in soil moisture content of a grid element is a function of the soil moisture content in the adjacent grid elements. The importance of (x) is in satisfying the underlying assumptions of the Kalman-filter, and hence ensuring stable updating of the forecasting equation.

7.2 APPLICABILITY OF EXISTING MODELS

Hydrological models can be classified into three groups: (i) black box; (ii) conceptual; and (iii) process (Chiew *et al.,* 1993).

- In the black box modelling approach, empirical equations are used to relate rainfall and runoff, with only the input (rainfall) and output (runoff) having any physical meaning. Hence black box hydrologic models are of limited use in modelling soil moisture profiles.

- Conceptual models have more physical meaning than black box models, but are simpler than process models. In the conceptual model, a catchment is conceptualised as consisting of a number of interconnected storages, with

mathematical functions to describe the movement of water into, between and out of them. These models attempt to represent the catchment physical processes but often include empirical equations. In conceptual models, soil moisture content is often modelled by a single soil layer. Hence these models are of limited use in modelling soil moisture.

- Process models are at the cutting edge of technology, in that they attempt to simulate the hydrological processes in a catchment and involve the use of many partial differential equations governing various physical processes and equations of continuity for surface water and soil moisture flow.

When choosing a hydrologic model, it is necessary to identify the key processes that are active in the catchment under consideration, and ensure that they are satisfactorily represented by the model (Hughes, 1994). In the Nerrigundah experimental catchment (Chapter 9), which is a typical catchment for temperate regions, soil is rather thin and overlays very low permeability sandstone. Hence, at least for the majority of the catchment, there is no permanent water table (but a water table may form during wet periods, particularly in the convergent zones) and there is essentially zero moisture flux from the soil into the sandstone. Furthermore, vertical rise of soil moisture from deeper layers to the soil surface is an important feature of the Nerrigundah catchment, which must be accounted for in the hydrologic model. While many real soils have significant crack or other macro-pore systems (Kirkby, 1985), this has not been identified in the Nerrigundah catchment, and consequently will not be modelled.

A limitation of many existing hydrologic models is their emphasis on runoff estimation (eg. Beven and Kirkby, 1979; Boughton, 1983; Ottlé and Vidal-Madjar, 1994; Moore and Grayson, 1991; Wood *et al.,* 1992), and poor representation of the soil moisture profile. Furthermore, those models accounting for soil moisture more explicitly often have restrictive assumptions, such as:

- The existence of a water table for the lower boundary condition (eg. Famiglietti *et al.*, 1992; Famiglietti and Wood, 1994a,b).
- That the water table is very deep (Rao *et al*., 1990; Lakshmi *et al*., 1997).

- That there is no lateral redistribution between grid elements (Groves, 1989; Ottlé *et al*., 1989; Capehart and Carlson, 1994).
- That all rainfall enters the soil until saturation (Wigmosta *et al*., 1994).
- That soil moisture can be modelled with only two soil layers (Beven and Kirkby, 1979; Ottlé *et al*., 1989; Liang *et al.*, 1994; Hughes and Sami, 1994; Wigmosta *et al*., 1994; Lakshmi *et al*., 1997).
- That there is a uniform soil moisture profile at the start of storm and inter-storm periods (Eagleson, 1978; Groves, 1989).
- That there is gravity drainage but no capillary rise to recharge the near-surface layer(s) (Beven and Kirkby, 1979; Cabral *et al*., 1992; Liang *et al*., 1994; Wigmosta *et al*., 1994).

Of those models that do account for capillary rise, which has been shown by Liang *et al*. (1996) to be important in achieving realistic results for low soil moisture contents, the Richards equation has generally been applied with the assumption that it is applicable for a large vertical discretisation (eg. Liang *et al*., 1996; Lakshmi *et al.*, 1997). In addition, discretisation of the horizontal model domain is often not compatible with the observation domain (eg. Moore and Grayson, 1991) or not comparable with the observations (eg. Beven and Kirkby, 1979; Wood *et al.,* 1992; Hughes and Sami, 1994) as the soil moisture distribution is modelled statistically.

While the three-dimensional Richards equation can be used to model soil moisture content on a regular grid without the restrictive assumptions identified above (eg. Paniconi and Wood, 1993), its application is computationally demanding. Hence, the development of a computationally efficient hydrologic model for the purpose of modelling soil moisture in the Nerrigundah catchment has been essential, in order to satisfy the requirements of the forecasting model for the soil moisture profile estimation algorithm, and to overcome the limiting assumptions and restrictions of existing models.

The following section describes the catchment scale soil moisture model ABDOMEN (**A**pproximate **B**uckingham-**D**arcy equati**O**n for **M**oisture **E**stimatio**N**), which was used for forecasting of the soil moisture profiles in the

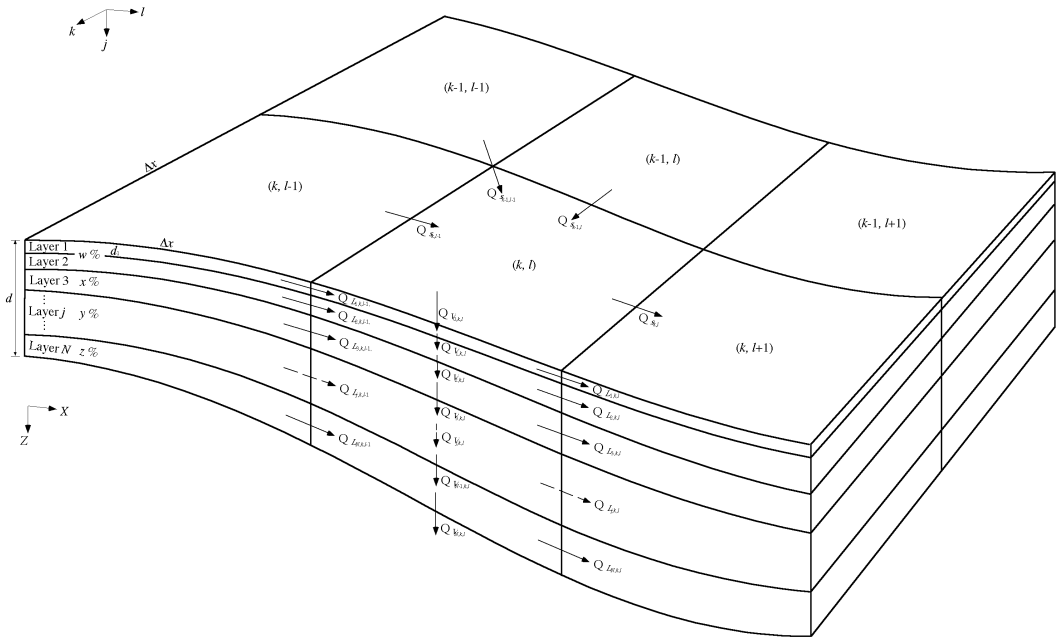

Figure 7.1: Schematic representation of the catchment scale soil moisture model ABDOMEN3D.

field applications of the soil moisture profile estimation algorithm (Chapter 10 and Chapter 11). This model uses an implicit solver for predicting soil moisture content from an approximate form of the Buckingham-Darcy equation. A complete listing of the one-dimensional (ABDOMEN1D) and three-dimensional (ABDOMEN3D) versions of the computer code are given on the CD-ROM accompanying this thesis.

7.3 ABDOMEN MODEL DEVELOPMENT

A schematic representation of the distributed soil moisture profile model is given in Figure 7.1. Layer 1 is of constant thickness over the entire catchment and is commensurate with the remote sensing observation depth. A minimum of one additional layer is then required for modelling the time variation of soil moisture content in the remainder of the soil profile. As soil depth varies across a catchment, these lower layers must be of varying thickness in order to maintain the same number of soil layers. The layer thickness is thus modelled by specifying a fixed proportion of the lower profile depth for each layer.

Surface runoff Q_s is modelled only when the ponding depth *POND* exceeds the depression storage depth *DEPSTR*, and is modelled using the

Manning equation (Streeter and Wylie, 1983). Runoff from each grid element is allowed in any one of the eight directions, whichever is the maximum downslope direction.

The difficulty associated with satisfying the requirement of simplicity and minimal computation effort, is in estimating the vertical Q_V and lateral Q_L soil moisture fluxes. Unsaturated flow through porous media can be described by the Buckingham-Darcy equation as

$$Q = K\nabla(\psi + z) \qquad (7.1),$$

where Q is the volumetric flux of liquid water positive downwards, K is the unsaturated hydraulic conductivity, ∇ is the gradient operator, ψ is the matric suction (ie. opposite sign to matric head) and z is the elevation positive downwards. The reverse sign notation used here for ψ and z as compared to Chapter 5 is to simplify the equations in the subsequent model development. The unsaturated hydraulic conductivity can be estimated from the Brooks and Corey (1966), Clapp and Hornberger (1978) or van Genuchten (1980) models given in section 5.2.3.

The Buckingham-Darcy equation can be written as

$$Q_V = K\frac{\partial\psi}{\partial Z} + K\frac{\partial z}{\partial Z} \qquad (7.2a)$$

$$Q_L = K\frac{\partial\psi}{\partial X} + K\frac{\partial z}{\partial X} \qquad (7.2b),$$

for the vertical (perpendicular to soil surface) and lateral (parallel to soil surface) directions respectively. The first right hand side term in these equations is a matric suction term which tends to move soil moisture towards areas of greater matric suction (lower soil moisture), whilst the second right hand side term accounts for gravity drainage. Thus, soil moisture can move upward against gravity during an exfiltration event if the matric suction term is greater than the gravity drainage

term. During an infiltration event, soil moisture can move downwards faster than for gravity drainage until saturation occurs.

7.3.1 CONCEPTUAL SOIL MOISTURE FLUX EQUATIONS

Accurate solution of the Buckingham-Darcy equation requires a fine spatial discretisation of the model domain, thus requiring a large computational effort. In addition, the Buckingham-Darcy equation requires knowledge of the ψ–θ relationship, adding complexity to the model. Therefore a simplified version of (7.2) is desired, such as the conceptual equations proposed in (7.3).

$$Q_V = K \cdot VDF + K \cdot (1 - SLOPE) \qquad (7.3a)$$

$$Q_L = K \cdot LDF + K \cdot SLOPE \qquad (7.3b),$$

where *VDF* and *LDF* are vertical and lateral distribution factors that can be used to describe the redistribution of soil moisture due to matric suction (equivalent to $\nabla\psi$ in (7.2)), whilst not modelling matric suction directly. In the strictest sense, *SLOPE* is the topographic slope between the midpoints of the soil layer (m m^{-1}) in the drainage direction (maximum downslope direction). However, for simplicity, *SLOPE* may be taken as the surface slope. Furthermore, this avoids the possibility of different layers in the same grid element draining to different grid elements. Hence, the catchment scale soil moisture model developed in this chapter is only a quasi three-dimensional model, with redistribution of soil moisture only occurring in two directions for any given grid element (ie, vertically and laterally in the maximum downslope direction). The unsaturated hydraulic conductivity *K* may be taken as the arithmetic average of the two elements for which the volumetric moisture flux is being estimated.

An appropriate form for *VDF* and *LDF* may be obtained by analysing the special cases given in Figure 7.2, using a totally conceptual approach. These special cases indicate that the distribution factors should be: (i) zero if adjacent elements have the same soil moisture content; (ii) positive if the upward element has a greater soil moisture content; (iii) negative if the downward element has a

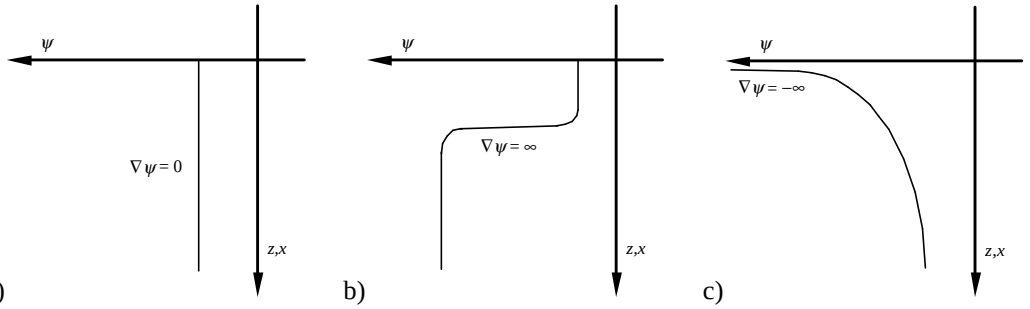

Figure 7.2: Typical matric head profiles: a) uniform; b) infiltration; and c) exfiltration.

greater soil moisture content; and (iv) approach ±∞ if the difference in moisture content of adjacent elements is great (assuming uniform soil properties).

7.3.1.1 Version 1 Distribution Factors

Based on the observations stated above, the simplest form for the distribution factors assuming uniform soil properties is

$$VDF = MGRAD\left(\frac{\theta_{j,k,l} - \theta_{j+1,k,l}}{\phi - \theta_r}\right) \qquad (7.4a)$$

$$LDF = MGRAD\left(\frac{\theta_{j,k,l} - \theta_{j,k+1,l}}{\phi - \theta_r}\right) \qquad (7.4b),$$

where *MGRAD* is a maximum gradient parameter, $\theta_{j,k,l}$ is the volumetric soil moisture of the *j,k,l*th element, ϕ is the soil porosity and θ_r is the residual soil moisture content. Using this conceptualisation, the bracketed term is: –1 when $\theta_{j,k,l}$ equals θ_r and $\theta_{j+1,k,l}$ equals ϕ; +1 when $\theta_{j,k,l}$ equals ϕ and $\theta_{j+1,k,l}$ equals θ_r; and 0 when $\theta_{j,k,l}$ equals $\theta_{j+1,k,l}$. Hence, the *MGRAD* term is used to scale the conceptual distribution factor from –∞ to +∞. However, it was found that this particular form of the distribution factors was discretisation dependent (see section 7.4.1.1).

7.3.1.2 Version 2 Distribution Factors

A more sophisticated formulation of the distribution factors, which is independent of the model discretisation is

$$VDF = \frac{MGRAD}{DZ}\left(\frac{\theta_{j,k,l} - \theta_{j+1,k,l}}{\phi - \theta_r}\right) \qquad (7.5a)$$

$$LDF = \frac{MGRAD}{DX}\left(\frac{\theta_{j,k,l} - \theta_{j,k+1,l}}{\phi - \theta_r}\right) \qquad (7.5b),$$

where DZ is the perpendicular distance between the midpoints of layer j and j+1 and DX is the lateral slope distance between the midpoints of grid cell k,l and k+1,l. By dividing the scaling factor MGRAD by the separation between element midpoints, the tendency for redistribution of soil moisture content is reduced when the separation is increased. Although both the version 1 and version 2 distribution factors correspond with the typical matric head profiles of Figure 7.2, they do not account for the non-linearity of $\partial\psi/\partial Z$ with θ (see section 7.4.1.2).

7.3.1.3 Version 3 Distribution Factors

A final formulation for the distribution factors that incorporates the matric head non-linearity with soil moisture content (see section 7.4.1.3) is

$$VDF = \frac{MGRAD}{\left(\theta_{j+\frac{1}{2},k,l} - \theta_r\right)^2 DZ}\left(\frac{\theta_{j,k,l} - \theta_{j+1,k,l}}{\phi - \theta_r}\right) \qquad (7.6a)$$

$$LDF = \frac{MGRAD}{\left(\theta_{j,k+\frac{1}{2},l} - \theta_r\right)^2 DX}\left(\frac{\theta_{j,k,l} - \theta_{j,k+1,l}}{\phi - \theta_r}\right) \qquad (7.6b),$$

where $\theta_{j+1/2,k,l}$ is the average soil moisture for layer j and j+1 of grid cell k,l and $\theta_{j,k+1/2,l}$ is the average soil moisture for grid cell k,l and k+1,l of layer j. Dividing the scaling term by the soil moisture content term results in a greater tendency for redistribution of moisture at low soil moisture content, and a lower tendency for redistribution of moisture at high soil moisture content. This is in keeping with the usual moisture retention relationships, which have a non-linear dependence of matric suction with soil moisture content, particularly at low soil moisture contents.

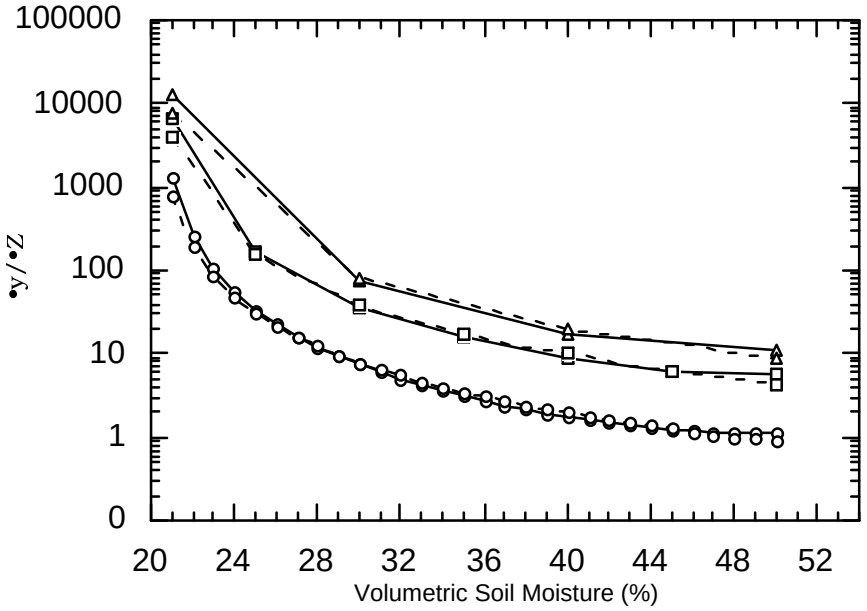

Figure 7.3: Comparison of the version 3 distribution factor (dashed line) with $\partial\psi/\partial Z$ from the van Genuchten (1980) relationship (solid line) for three different $\Delta\theta$ with a given separation Δz of 10 cm: 1% v/v (circle), 5% v/v (square) and 10% v/v (triangle).

A comparison of the version 3 vertical distribution factor with $\partial\psi/\partial Z$ from the van Genuchten (1980) relationship is given in Figure 7.3 for the soil parameters in Table 7.1. This figure shows a very good comparison, with the exception of soil moisture content values close to the residual soil moisture content and soil porosity values, and is obviously a great improvement (in terms of representing the Richards equation) on the version 2 distribution factor, which would plot as a horizontal line.

7.3.1.4 Inhomogeneous Version 3 Distribution Factors

To account for spatial heterogeneity in soil properties (residual soil moisture content and soil porosity), the version 3 distribution factors in (7.6) can be written as

$$VDF = GRAD_{j+\frac{1}{2},k,l}\left(\frac{\theta_{j,k,l}-\theta_{r_{j,k,l}}}{\phi_{j,k,l}-\theta_{r_{j,k,l}}}-\frac{\theta_{j+1,k,l}-\theta_{r_{j+1,k,l}}}{\phi_{j+1,k,l}-\theta_{r_{j+1,k,l}}}\right) \qquad (7.7a)$$

Table 7.1: Soil parameters used for evaluation of the version 3 vertical distribution factor and $\partial\psi/\partial Z$ in Figure 7.3.

Residual Soil Moisture Content θ_r	20% v/v
Soil Porosity ϕ	54% v/v
Van Genuchten Parameter η	0.008
Van Genuchten Parameter n	1.8
Soil Discretisation Δz	10 cm
Maximum Gradient Parameter *MGRAD*	27 cm

$$LDF = GRAD_{j,k+\frac{1}{2},l}\left(\frac{\theta_{j,k,l}-\theta_{r_{j,k,l}}}{\phi_{j,k,l}-\theta_{r_{j,k,l}}}-\frac{\theta_{j,k+1,l}-\theta_{r_{j,k+1,l}}}{\phi_{j,k+1,l}-\theta_{r_{j,k+1,l}}}\right) \qquad (7.7b),$$

where

$$GRAD_{j+\frac{1}{2},k,l}=\frac{0.5}{DZ}\left(\frac{MGRAD_{j,k,l}+MGRAD_{j+1,k,l}}{\left(\theta_{j,k,l}-\theta_{r_{j,k,l}}\right)^2+\left(\theta_{j+1,k,l}-\theta_{r_{j+1,k,l}}\right)^2}\right) \quad (7.8a)$$

$$GRAD_{j,k+\frac{1}{2},l}=\frac{0.5}{DX}\left(\frac{MGRAD_{j,k,l}+MGRAD_{j,k+1,l}}{\left(\theta_{j,k,l}-\theta_{r_{j,k,l}}\right)^2+\left(\theta_{j,k+1,l}-\theta_{r_{j,k+1,l}}\right)^2}\right) \quad (7.8b).$$

The difference between the distribution factors presented in (7.7) and those in (7.6) is that there may be a different residual soil moisture content, soil porosity and/or maximum gradient parameter for each grid element.

A distribution factor of this form has been used, as it reduces to the distribution factors in (7.6) when adjacent grid elements have the same soil properties. These are the distribution factors used in the field application studies in Chapters 10 and 11.

7.3.1.5 Soil Moisture Flux Equations

The conceptual volumetric soil moisture flux equations can be vectorised for the vertical and lateral fluxes as

$$Q_{V_{j,k,l}} = \left\langle \frac{GRAD_{j+\frac{1}{2},k,l} \cdot K_{j+\frac{1}{2},k,l}}{\left(\phi_{j,k,l} - \theta_{r_{j,k,l}}\right)}, \quad -\frac{GRAD_{j+\frac{1}{2},k,l} \cdot K_{j+\frac{1}{2},k,l}}{\left(\phi_{j+1,k,l} - \theta_{r_{j+1,k,l}}\right)} \right\rangle \begin{Bmatrix} \theta_{j,k,l} \\ \theta_{j+1,k,l} \end{Bmatrix} + \left\langle \begin{matrix} K_{j+\frac{1}{2},k,l} \cdot (1 - SLOPE) - \\ GRAD_{j+\frac{1}{2},k,l} \cdot K_{j+\frac{1}{2},k,l} \left(\frac{\theta_{r_{j,k,l}}}{\phi_{j,k,l} - \theta_{r_{j,k,l}}} + \frac{\theta_{r_{j+1,k,l}}}{\phi_{j+1,k,l} - \theta_{r_{j+1,k,l}}} \right) \end{matrix} \right\rangle \quad (7.9a)$$

$$Q_{L_{j,k,l}} = \left\langle \frac{GRAD_{j,k+\frac{1}{2},l} \cdot K_{j,k+\frac{1}{2},l}}{\left(\phi_{j,k,l} - \theta_{r_{j,k,l}}\right)}, \quad -\frac{GRAD_{j,k+\frac{1}{2},l} \cdot K_{j,k+\frac{1}{2},l}}{\left(\phi_{j,k+1,l} - \theta_{r_{j,k+1,l}}\right)} \right\rangle \begin{Bmatrix} \theta_{j,k,l} \\ \theta_{j,k+1,l} \end{Bmatrix} + \left\langle \begin{matrix} K_{j,k+\frac{1}{2},l} \cdot SLOPE - \\ GRAD_{j,k+\frac{1}{2},l} \cdot K_{j,k+\frac{1}{2},l} \left(\frac{\theta_{r_{j,k,l}}}{\phi_{j,k,l} - \theta_{r_{j,k,l}}} + \frac{\theta_{r_{j,k+1,l}}}{\phi_{j,k+1,l} - \theta_{r_{j,k+1,l}}} \right) \end{matrix} \right\rangle \quad (7.9b),$$

where

$$K_{j+\frac{1}{2},k,l} = \frac{K_{j,k,l} + K_{j+1,k,l}}{2} \quad (7.10a)$$

$$K_{j,k+\frac{1}{2},l} = \frac{K_{j,k,l} + K_{j,k+1,l}}{2} \quad (7.10b),$$

by substitution of the version 3 distribution factors in (7.6) into the conceptual soil moisture flux equations in (7.3). The model parameter *K* (unsaturated hydraulic conductivity) and the distribution factor term *GRAD* are estimated from the soil moisture contents for the current time step.

7.3.2 THE GLOBAL SOIL MOISTURE EQUATION

To illustrate how the conceptual soil moisture flux equations in (7.9) may be used to assemble the global soil moisture equation, consider a single model

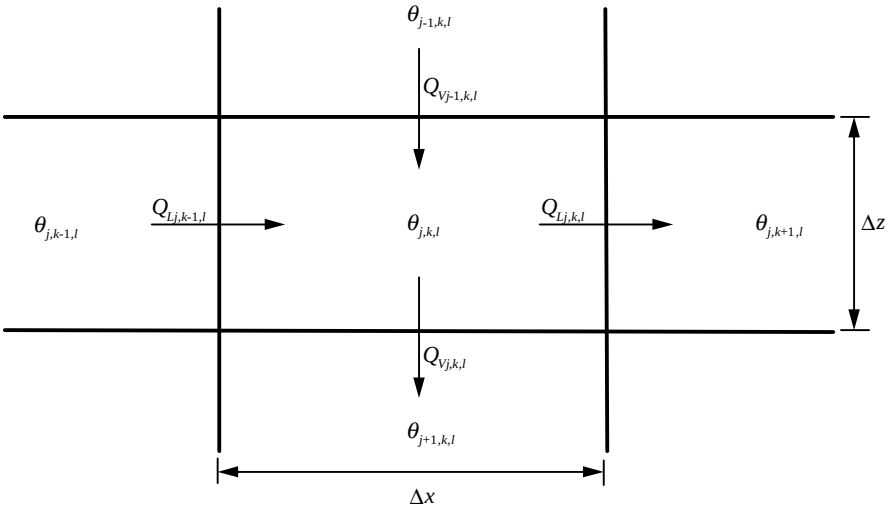

Figure 7.4: Schematic of water balance for a single grid element in the catchment with flow in two dimensions only.

element with unsaturated flow in two dimensions (Figure 7.4). By applying the continuity equation, the time variation of soil moisture content for element *j,k,l* is

$$\theta_{j,k,l}^{n+1} = \theta_{j,k,l}^{n} + \left[Q_{V_{j-1,k,l}} - Q_{V_{j,k,l}}\right]\frac{\Delta t}{\Delta z} + \left[Q_{L_{j,k,l-1}} - Q_{L_{j,k,l}}\right]\frac{\Delta t}{\Delta x} \qquad (7.11),$$

where Δt is the time step size, Δz is the layer thickness and Δx is the grid element length.

In order to apply (7.11) to a boundary element, additional information is required to estimate the soil moisture flux across the boundary. This information is referred to as the boundary condition, which may be either a Dirichlet (fixed soil moisture content for the boundary element) or Neumann (specified soil moisture flux across the boundary) condition. If the volumetric flux across the base of the bottom soil layer is known, then this may be applied directly. More commonly however, particularly for a deep soil, gravity drainage is assumed across the base of the bottom soil layer ($Q_V = K_{N,k,l}$). If it is desired to model a water table at the base of the soil column, then an imaginary soil layer may be applied below the bottom soil layer with zero thickness and fixed soil moisture content equal to the porosity of the bottom soil layer. The vertical flux across the bottom soil layer boundary may then be estimated from (7.9a).

Likewise, if there is an infiltration event, the infiltration rate (limited by the actual precipitation rate and ponding depth) may be estimated by applying an imaginary soil layer above the soil surface of zero thickness and soil moisture equal to the porosity of the near-surface soil layer. This makes the assumption that there is zero matric head at the soil surface, which in reality is equal to the ponding depth. However, providing the ponding depth is not great, this has a negligible influence on estimation of the infiltration rate in practical applications.

If there is an exfiltration event, then the actual evapotranspiration rate may be applied directly, or estimated from the soil moisture content and potential evapotranspiration rate using a soil moisture stress index.

The lateral soil moisture flux at the catchment outlet is estimated by assuming only gravity drainage occurs, as there is no knowledge of the soil moisture content of the downhill grid cell. Moreover, soil moisture contents at the catchment outlet are often high, meaning that capillary effects will be minimal.

The mass balance for each of the grid elements is ensured by upwelling any forecast soil moisture storage in excess of the soil porosity to the soil layer above. Starting from the lowest soil layer in each grid cell, this procedure is repeated until there is no longer a soil moisture storage forecast in excess of the soil porosity, or the soil surface is reached. If the soil surface is reached, the forecast soil moisture storage excess is added to the ponding depth, and is available for runoff if the ponding depth exceeds the depression storage.

7.3.3 APPLICATION TO THE KALMAN-FILTER

The Kalman-filter assimilation scheme requires the soil moisture profile forecasting equation to be in the explicit form of (3.1). However, explicit models can only take small time steps, and hence run much more slowly than implicit models. On the other hand, implicit models require iteration until convergence at each time step. As computation time was a major limitation with the one-dimensional explicit model PROXSIM1D, which was described in Chapter 5, a variant of the implicit scheme was used. If we write (7.11) in terms of the Crank-Nicholson implicit scheme (Gerald and Wheatley, 1989), then

$$\theta_{j,k,l}^{n+1} - \frac{1}{2}\left(\begin{matrix} \left[Q_{V_{j-1,k,l}} - Q_{V_{j,k,l}}\right]\frac{\Delta t}{\Delta z} \\ + \left[Q_{L_{j,k,l-1}} - Q_{L_{j,k,l}}\right]\frac{\Delta t}{\Delta x} \end{matrix} \right)^{n+1} = \theta_{j,k,l}^{n} + \frac{1}{2}\left(\begin{matrix} \left[Q_{V_{j-1,k,l}} - Q_{V_{j,k,l}}\right]\frac{\Delta t}{\Delta z} \\ + \left[Q_{L_{j,k,l-1}} - Q_{L_{j,k,l}}\right]\frac{\Delta t}{\Delta x} \end{matrix} \right)^{n} \quad (7.12).$$

Substituting for Q from (7.9) and assembling the global soil moisture state equation we can obtain an equation of the form

$$\mathbf{\Phi}_1^{n+1} \cdot \hat{\mathbf{X}}^{n+1/n} + \mathbf{\Omega}_1^{n+1} = \mathbf{\Phi}_2^{n} \cdot \hat{\mathbf{X}}^{n/n} + \mathbf{\Omega}_2^{n} \quad (7.13).$$

After some algebraic manipulation of (7.13) we can obtain the linear state space equation

$$\hat{\mathbf{X}}^{n+1/n} = \mathbf{A}^{n} \cdot \hat{\mathbf{X}}^{n/n} + \mathbf{U}^{n} \quad (7.14),$$

where

$$\mathbf{A}^{n} = \left[\mathbf{\Phi}_1^{n+1}\right]^{-1} \cdot \left[\mathbf{\Phi}_2^{n}\right] \quad (7.15a)$$

$$\mathbf{U}^{n} = \left[\mathbf{\Phi}_1^{n+1}\right]^{-1} \cdot \left[\mathbf{\Omega}_2^{n} - \mathbf{\Omega}_1^{n+1}\right] \quad (7.15b),$$

being the explicit form required by the Kalman-filter (3.1). Once convergence of (7.13) has been achieved, the system state covariances may be forecast using the converged value for **A** from (7.15a). Using this approach, iteration is performed only for forecasting of the system states, with evaluation of **A** and forecasting of the system state covariances performed only once (after convergence of the system states), using a single large time step. As forecasting of the system state covariance matrix is computationally the most demanding step of the Kalman-filter (see section 3.3.2), this implicit approach minimises the computational effort required to forecast the system state covariances by the Kalman-filter forecasting equation (3.2).

7.3.4 TIME STEPPING PROCEDURE

The size of the computational time step used by the model can be determined automatically by a procedure that limits the magnitude of changes in the state variable to some specified value. The procedure presented here is similar to that suggested by Milly (1982) for a fully implicit backward difference scheme (see Chapter 5). Firstly, the maximum change in soil moisture for the previous time step is defined as

$$\varepsilon_\theta^{\,n} = \max_{j,k,l} \left| \theta^{\,n}_{j,k,l} - \theta^{\,n-1}_{j,k,l} \right| \qquad (7.16a).$$

Secondly, given a specified target for maximum change in soil moisture content in any element of the soil model domain of $\hat{\varepsilon}_\theta$, the new time step size can be forecast according to the rule

$$(\Delta t)^{n+1} = (\Delta t)^n \, \frac{\hat{\varepsilon}_\theta}{\varepsilon_\theta^{\,n}} \qquad (7.16b).$$

7.4 ABDOMEN MODEL EVALUATION

The simplified soil moisture model ABDOMEN was evaluated for two cases: (i) a one-dimensional soil column (using ABDOMEN1D), and (ii) a planar catchment (using ABDOMEN3D). The one-dimensional soil column was evaluated against simulation results from the one-dimensional soil moisture profile model presented in Chapter 5 (PROXSIM1D), while the results from modelling the planar catchment were evaluated against an analytical solution. The planar catchment consists of a two-dimensional hillslope of uniform slope and soil thickness.

7.4.1 ONE-DIMENSIONAL SOIL PROFILE

To verify the form of the conceptually based distribution factors proposed in the previous section, a comparison was made for a one-dimensional soil profile with the one-dimensional Richards equation model PROXSIM1D. The simulation

was for the same 1 m soil column used in the synthetic study of Chapter 6, with the soil properties listed in Table 6.1. Starting from an initially uniform soil moisture profile of 51.5% v/v (–50 cm matric head), the soil moisture profile was subjected to a constant evaporation rate of 0.5 cm day^{-1}, for 25 days.

7.4.1.1 Version 1 Distribution Factor

Using the version 1 distribution factor, the *MGRAD* parameter was determined by calibrating ABDOMEN1D to the PROXSIM1D simulations with the Bayesian non-linear regression program NLFIT (*MGRAD* = 152.5). The program suite NLFIT is an interactive optimisation package, employing the SCE-UA (**S**huffled **C**omplex **E**volution Method developed at The **U**niversity of **A**rizona) of Duan *et al.* (1994).

The soil moisture profile simulation results from this calibration are given in Figure 7.5, where a reasonably good agreement is seen between the PROXSIM1D and ABDOMEN1D models until about day 20, when the ABDOMEN1D simulation began to dry too rapidly near the soil surface. This was

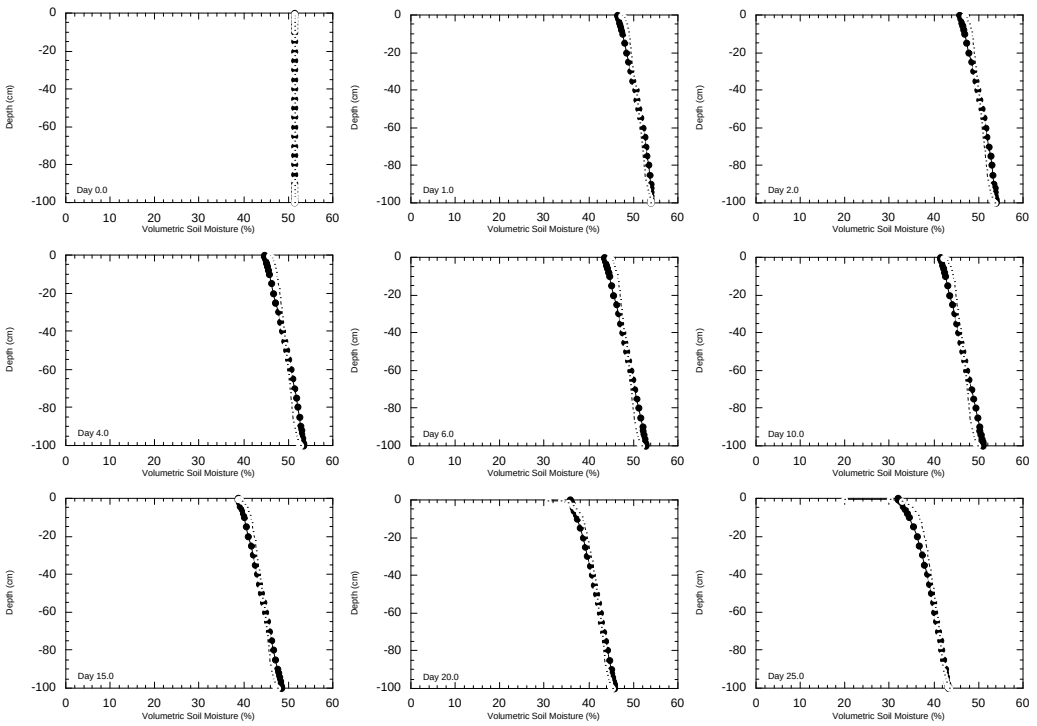

Figure 7.5: Comparison of simulated soil moisture profiles using ABDOMEN1D with the version 1 distribution factor (open symbols) and PROXSIM1D (closed symbols) for evaporation of 0.5 cm day^{-1}.

due to the extreme non-linearity in the ψ–θ relationship as the soil moisture content approached the residual soil moisture content, whilst the proposed distribution factor was linear. Of more concern however, was the consistent reverse S shape of soil moisture profiles from ABDOMEN1D. The reason for this was that soil layers at both ends of the soil column were thinner than those layers in the middle, which had constant thickness.

7.4.1.2 Version 2 Distribution Factor

To overcome the discretisation dependence of the version 1 distribution factor, the version 2 distribution factor was employed. This reduced the maximum gradient of internal layers and hence the volumetric moisture flux, whilst increasing the gradient of boundary layers (and the volumetric moisture flux), straightening the soil moisture profile and increasing the volumetric flux of soil moisture to the soil surface.

The *MGRAD* parameter for the version 2 distribution factor was again evaluated by calibrating to the PROXSIM1D simulations with NLFIT

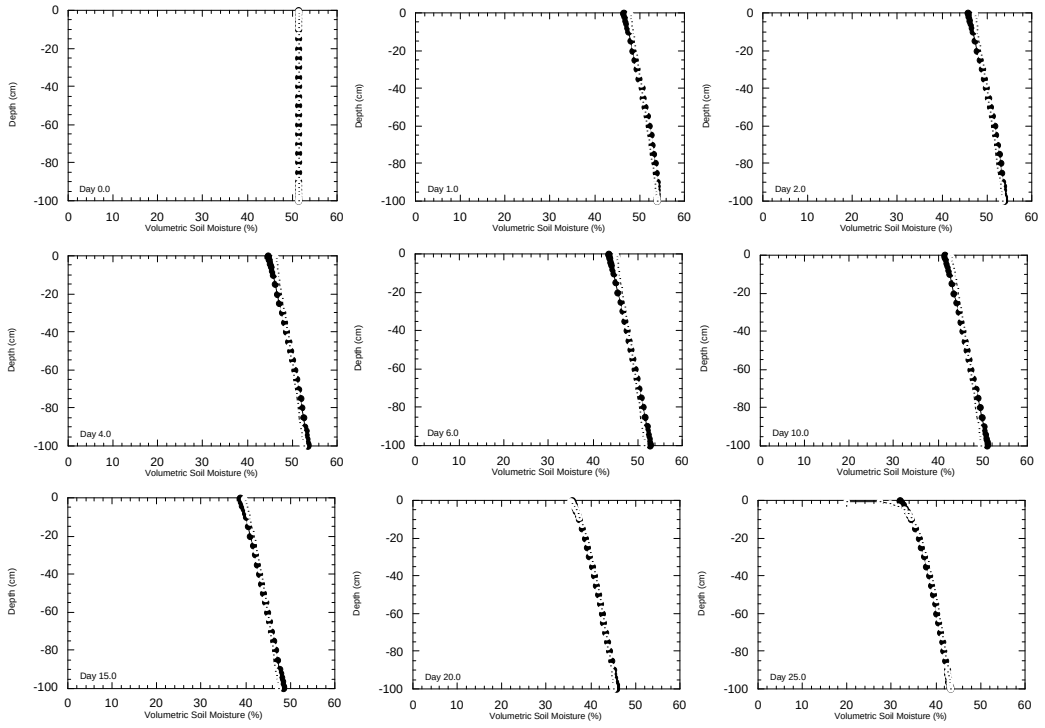

Figure 7.6: Comparison of simulated soil moisture profiles using ABDOMEN1D with the version 2 distribution factor (open symbols) and PROXSIM1D (closed symbols) for evaporation of 0.5 cm day^{-1}.

(*MGRAD* = 5842 mm). The results of this modification are given in Figure 7.6, where an even better agreement between ABDOMEN1D and PROXSIM1D is displayed. However, at early simulation times during the dry-down, the soil moisture profile simulations from ABDOMEN1D had a steeper gradient then those from PROXSIM1D. This was a result of fitting to the drier profiles. If calibration had only been performed for the first 15 days of the drying sequence, then the *MGRAD* parameter would be reduced and earlier profiles would be in better agreement.

7.4.1.3 Version 3 Distribution Factor

Whilst quite good agreement was achieved between the PROXSIM1D and ABDOMEN1D models with the version 2 distribution factor until day 20, there was a significant departure from the PROXSIM1D simulation for surface layers at day 25. As alluded to in the model development section, this was a result of the non-linearity of $\partial\psi/\partial Z$ with θ. As the soil becomes drier, the distribution factor should be greater for the same difference in soil moisture between the two soil layers. To overcome this, the version 3 distribution factor was proposed, which accounts for the actual soil moisture status. The effect of this was to increase the distribution factor at low soil moisture content and decrease the distribution factor at high soil moisture content, thus increasing the volumetric flux of soil moisture to the surface under dry conditions.

The *MGRAD* parameter for the version 3 distribution factor was evaluated from calibrating ABDOMEN1D to the PROXSIM1D simulations with NLFIT (*MGRAD* = 280 mm). The results from this calibration are given in Figure 7.7, where a very good agreement is displayed between the ABDOMEN1D and PROXSIM1D models for the entire 25 day period.

Without doing any further calibration, ABDOMEN1D (with version 3 distribution factor) and PROXSIM1D were compared for an infiltration event of 10 mm hr^{-1} precipitation, starting from a uniform initial condition of 25% v/v (–1362 cm matric head). The results from this 30 hour simulation in Figure 7.9 show an extremely good agreement for all simulation times, and are superior to

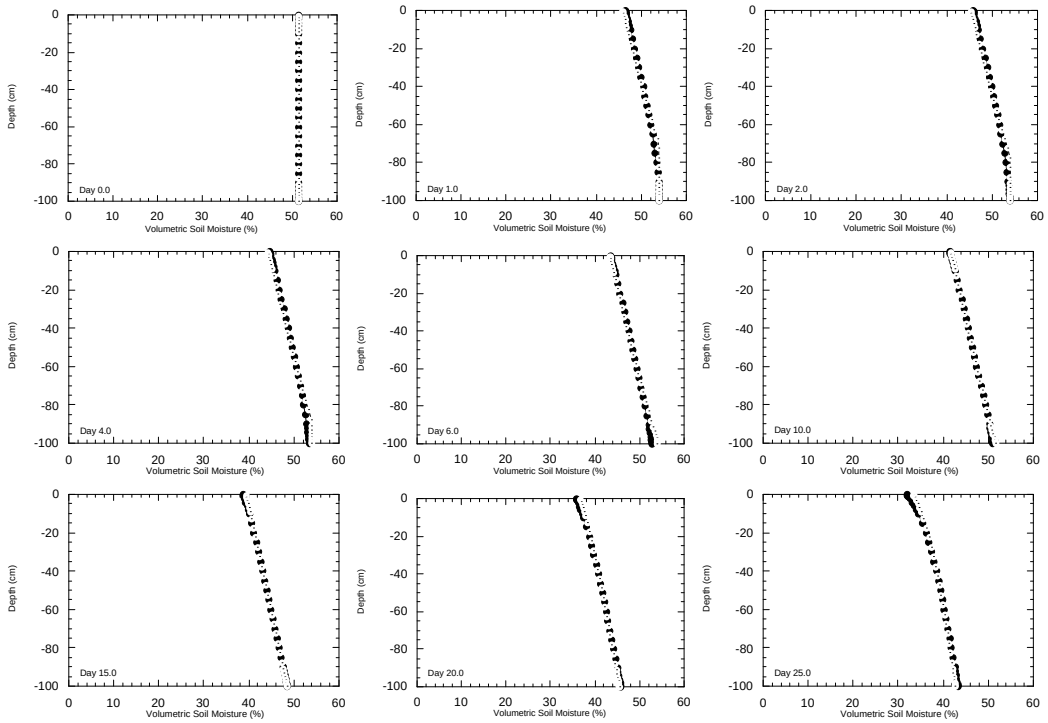

Figure 7.7: Comparison of simulated soil moisture profiles using ABDOMEN1D with the version 3 distribution factor (open symbols) and PROXSIM1D (closed symbols) for evaporation of 0.5 cm day^{-1}.

the results from ABDOMEN1D simulations with the version 2 distribution factor given in Figure 7.8.

The ultimate purpose of this simplified soil moisture model was to simulate soil moisture profiles with only a few soil layers. Whilst the simulations were very good for 30 layers, this may not be the case when only a few soil layers are used. Thus, the previous exfiltration and infiltration simulations with the version 3 distribution factor were repeated for 5 soil layers of increasing thickness, using the same *MGRAD* value as previously calibrated (280 mm). The ABDOMEN1D results from the exfiltration simulation (Figure 7.10) have shown the same good agreement with the PROXSIM1D simulations, with simulations essentially the same as for the 30 layer case.

The results from the infiltration simulation for 5 soil layers (Figure 7.11) have also shown a good agreement with the PROXSIM1D simulations, when taking into account layer thickness and that soil moisture content estimates are averages over the soil layer.

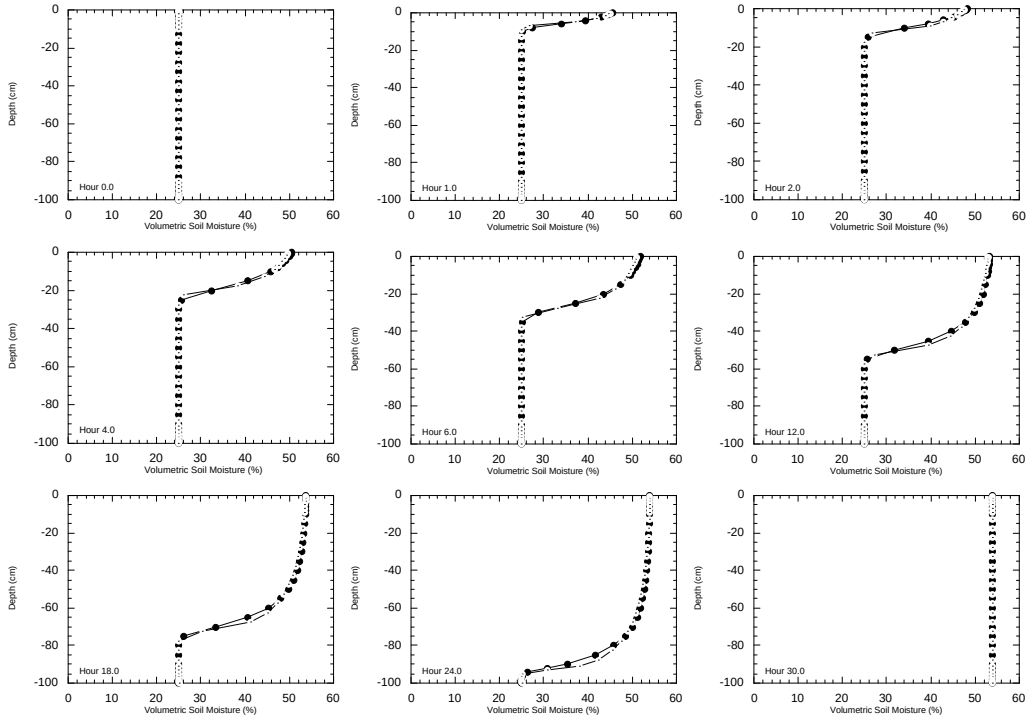

Figure 7.8: Comparison of simulated soil moisture profiles using ABDOMEN1D with the version 2 distribution factor (open symbols) and PROXSIM1D (closed symbols) for precipitation of 10 mm hr^{-1}.

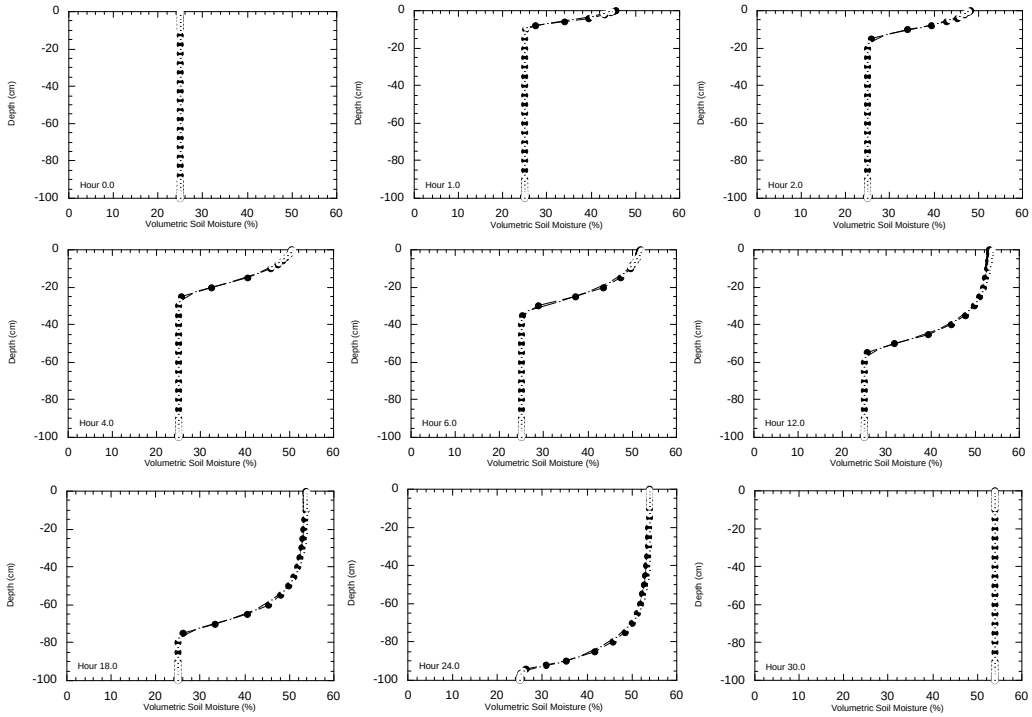

Figure 7.9: Comparison of simulated soil moisture profiles using ABDOMEN1D with the version 3 distribution factor (open symbols) and PROXSIM1D (closed symbols) for precipitation of 10 mm hr^{-1}.

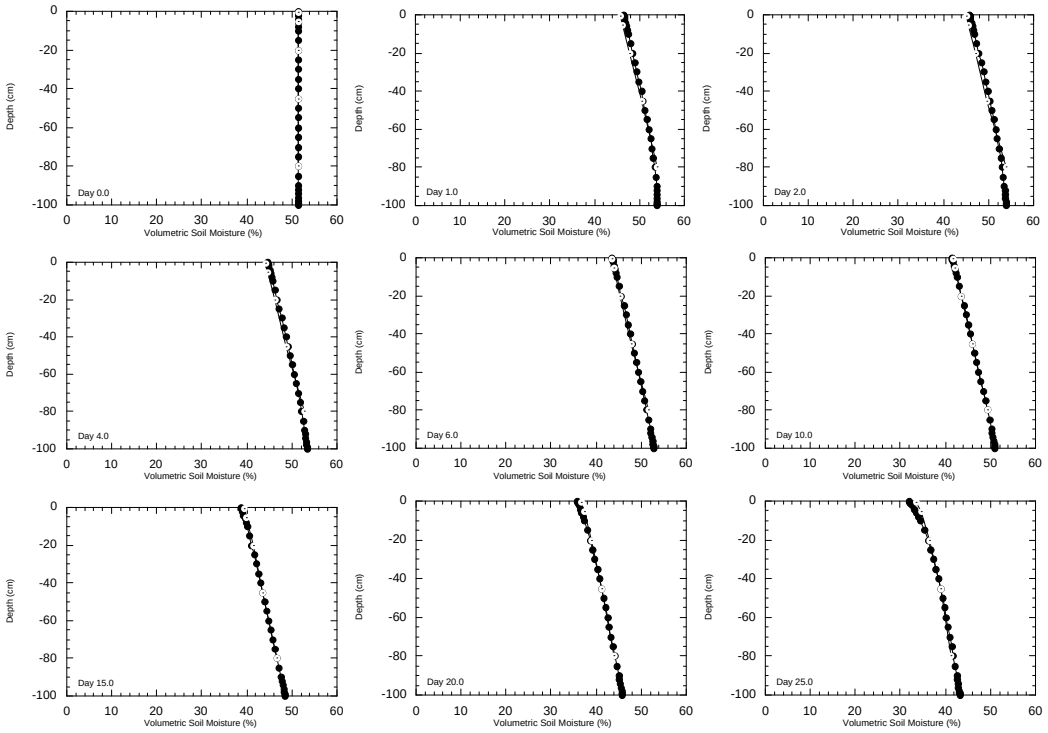

Figure 7.10: Comparison of simulated soil moisture profiles using ABDOMEN1D with the version 3 distribution factor for 5 soil layers (open symbols) and PROXSIM1D with 30 soil layers (closed symbols) for evaporation of 0.5 cm day^{-1}.

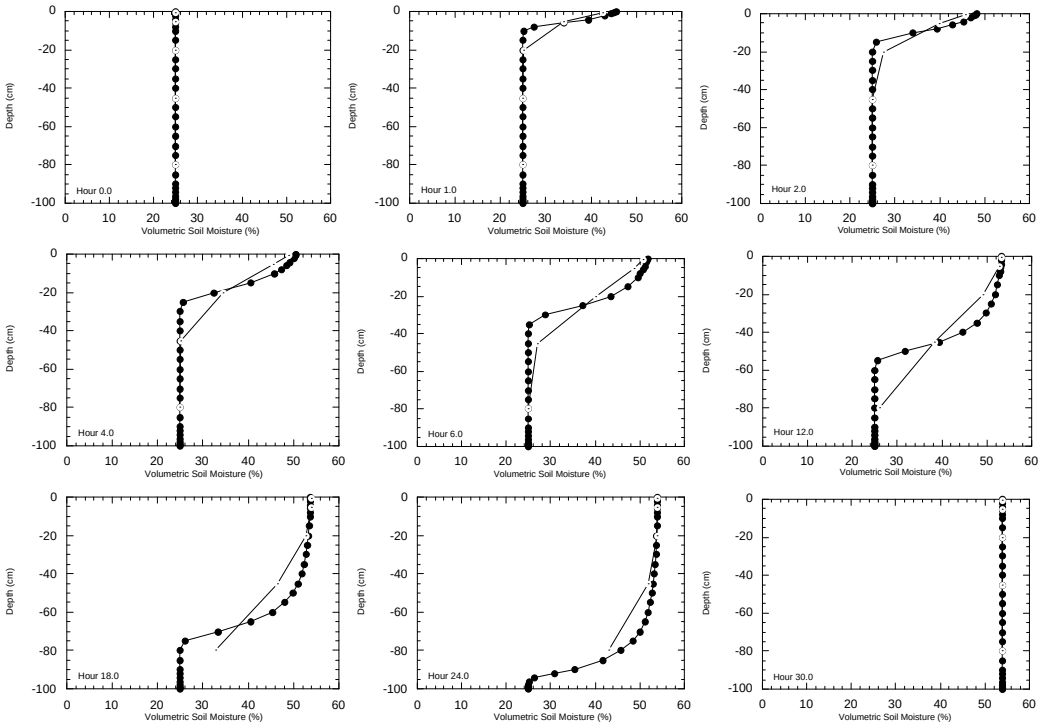

Figure 7.11: Comparison of simulated soil moisture profiles using ABDOMEN1D with the version 3 distribution factor for 5 soil layers (open symbols) and PROXSIM1D with 30 soil layers (closed symbols) for precipitation of 10 mm hr^{-1}.

7.4.1.4 Kalman-Filtering

Simulations in the previous section have shown that the simplified soil moisture profile model ABDOMEN1D (version 3 distribution factor) with only a few soil layers is an excellent approximation to the Richards equation. However, it has not yet been verified that the simplified soil moisture model is an appropriate forecasting model for the Kalman-filter assimilation scheme. Hence, the soil moisture profile estimation simulations used in the synthetic study of Chapter 6 were run with ABDOMEN1D (version 3 distribution factor) for observation intervals of 1 hour and 5 days.

Starting from the poor initial guess of 35.5% v/v, ABDOMEN1D was subjected to the constant evaporation rate of 0.5 cm day^{-1} and zero moisture flux at the column base. The model prediction was then updated with "observations" of the "true" soil moisture content in the top 1 cm layer. These observations were obtained from the "true" soil moisture profiles generated from PROXSIM1D. The results from these simulations with 29 soil layers are given in Figure 7.12 for updating once every hour and Figure 7.13 for updating once every five days. In these figures, the estimated soil moisture profiles are compared with the "open loop" simulation and the "true" soil moisture profiles from PROXSIM1D. The open loop simulation is where no "observations" were used and the system was simply propagated from the initial conditions subject to the surface flux boundary conditions.

Retrieval of the "true" soil moisture profile was obtained after the first update at hour 1 using ABDOMEN1D, compared with 12 hours for PROXSIM1D in the synthetic study of Chapter 6 (see Figure 6.8), for updating once every hour. However, for subsequent updates the estimated soil moisture profile did not follow the "true" soil moisture profile exactly, as was the case in Chapter 6. This was because the estimated and "true" soil moisture profiles were obtained from two different soil moisture profile models, rather than the same soil moisture profile model.

The Kalman-filter only has information about the near-surface soil layer and the depth correlation. Hence, it makes its adjustment of the soil moisture profile by fitting the model predictions to the observations (ie. the near-surface

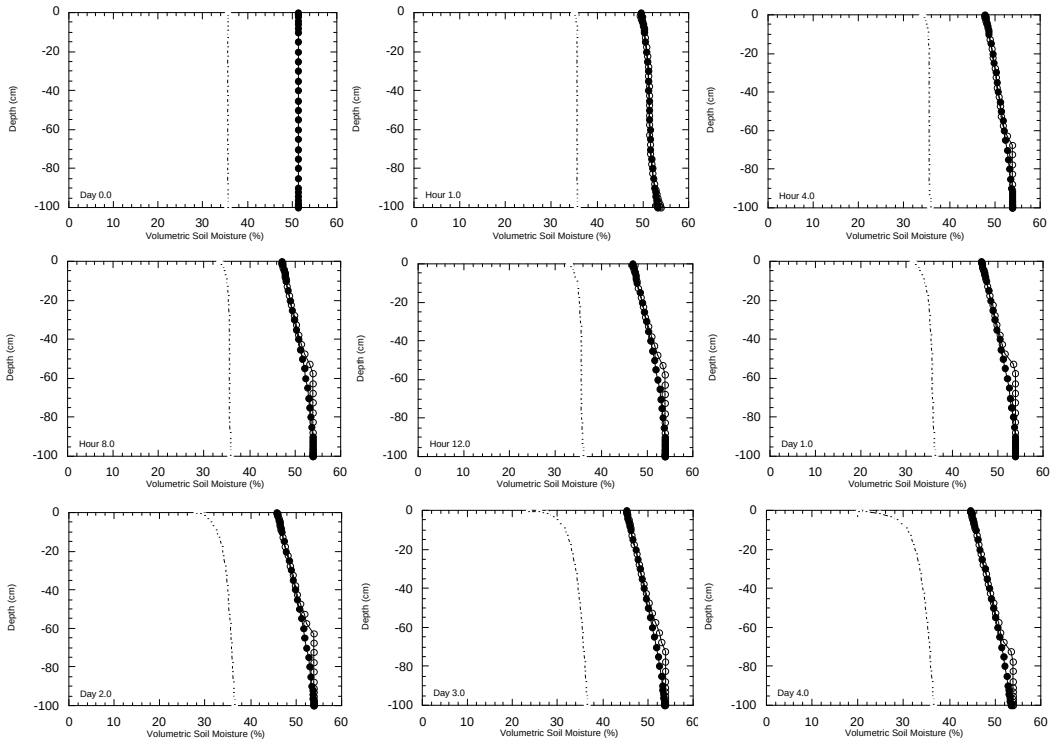

Figure 7.12: Comparison of soil moisture profile estimation using ABDOMEN1D with the version 3 distribution factor (open symbol), the open loop profile (open symbol with dot) and PROXSIM1D (closed symbol). The 29 layer model was updated once every hour using an observation depth of 1 cm; initial variances 0.25, system noise 5% of the state per hour and observation noise 2% of the state.

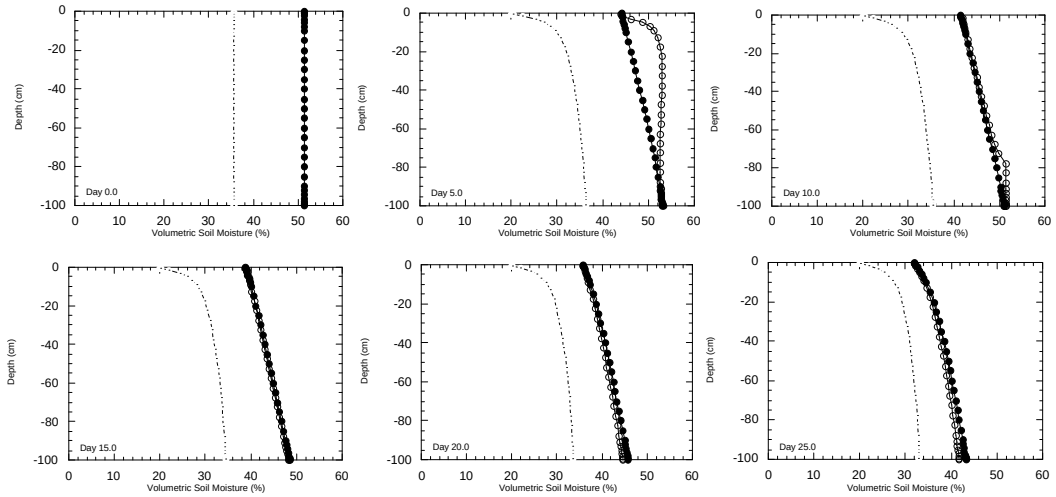

Figure 7.13: Comparison of soil moisture profile estimation using ABDOMEN1D with the version 3 distribution factor (open symbol), the open loop profile (open symbol with dot) and PROXSIM1D (closed symbol). The 29 layer model was updated once every hour using an observation depth of 1 cm; initial variances 0.25, system noise 5% of the state per hour and observation noise 2% of the state.

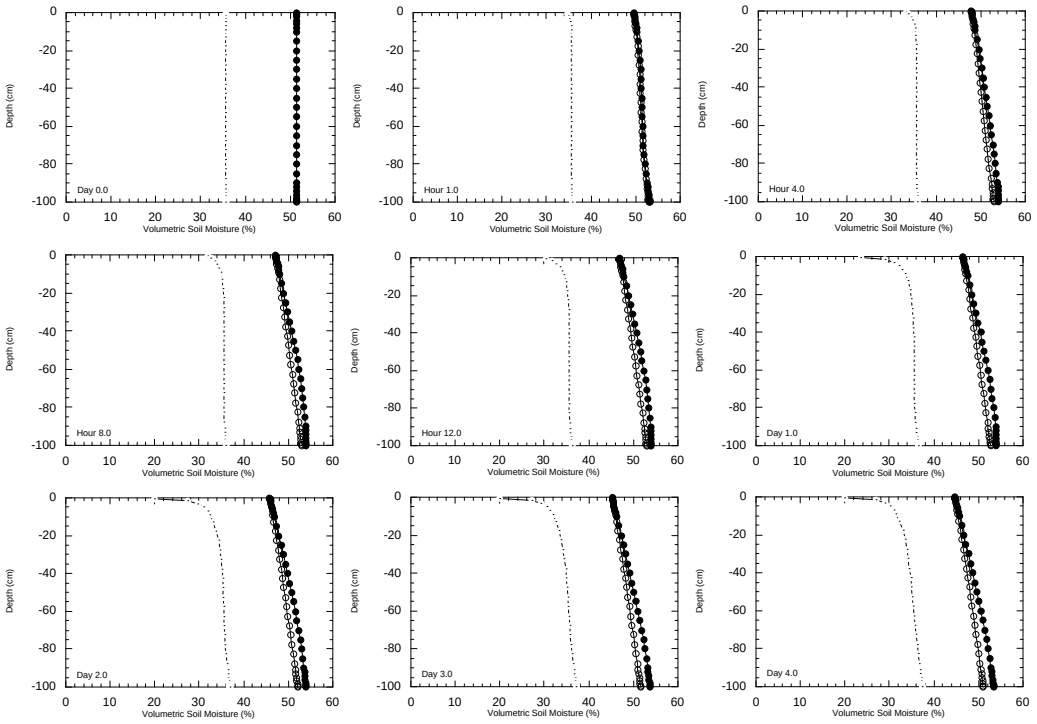

Figure 7.14: Comparison of soil moisture profile estimation using ABDOMEN1D with the version 2 distribution factor (open symbol), the open loop profile (open symbol with dot) and PROXSIM1D (closed symbol). The 29 layer model was updated once every hour using an observation depth of 1cm; initial variances 0.25, system noise 5% of the state per hour and observation noise 2% of the state.

layer). To further emphasise this, the Kalman-filter assimilation scheme was used to update ABDOMEN1D with the version 2 distribution factor from hourly "observations". The simulation results in Figure 7.14 showed once again that although retrieval of the "true" soil moisture profile was obtained at the first update (hour 1), the soil moisture profile estimation did not follow the "true" soil moisture profile exactly. It has already seen from Figure 7.6 that ABDOMEN1D (version 2 distribution factor) and PROXSIM1D did not agree exactly, with ABDOMEN1D having a steeper moisture gradient than PROXSIM1D. Thus, if we can imagine the soil moisture profile from ABDOMEN1D being shifted sideways to match the PROXSIM1D soil moisture content near the soil surface, a similar result to that from the Kalman-filter would be obtained. These differences between the estimated and "true" soil moisture profiles are likely to be indicative of the differences that will be obtained from field data, when the forecasting model does not capture the true dynamics of the soil moisture profile.

With updating once every 5 days, retrieval of the "true" soil moisture profile was obtained after only two updates (day 10), compared with 3 updates for

PROXSIM1D when using the soil moisture transformation (Figure 6.49). This confirms that modelling volumetric soil moisture as the dependent state leads to more stable updates of the soil moisture profile when using the Kalman-filter assimilation scheme.

As we planned to use the ABDOMEN model with only a few soil layers, we had to ensure that the updating characteristics seen in these simulations were evident in the case of a few soil layers. To confirm this, the two simulations above were repeated for 5 soil layers. The results from these simulations are given in Figure 7.15 for updating once every hour and Figure 7.16 for updating once every five days.

These simulation results have shown that the Kalman-filter assimilation scheme worked as well for 5 soil layers as it did for 29 soil layers. Hence, the proposed form of the version 3 distribution factor is such that strong correlations are being generated between the soil layers.

Whilst the simulations from updating every 5 days were essentially the same for both numbers of soil layers, retrieval of the "true" soil moisture profile from updating once every hour was longer for the 5 layer case, with retrieval of the "true" soil moisture profile taking approximately 12 hours. This retrieval time was more commensurate with that from the PROXSIM1D results in Chapter 6. The reason for soil moisture profile retrieval taking longer with 5 soil layers than for 29 soil layers is most likely due to the higher correlations between soil layers that are closer together, as in the 29 layer case, allowing the correlations between soil layers to build up more quickly.

7.4.2 PLANAR CATCHMENT

In order to test the lateral redistribution component of the simplified soil moisture profile model ABDOMEN3D, sub-surface discharge is compared with an analytical solution for a hypothetical planar catchment.

Based on the work of Henderson and Wooding (1964), Beven (1981) and Beven (1982), Perera (1998) has presented an analytical solution to the kinematic wave equation for estimation of the sub-surface discharge hydrograph from a planar catchment. The assumptions made in deriving this solution were:

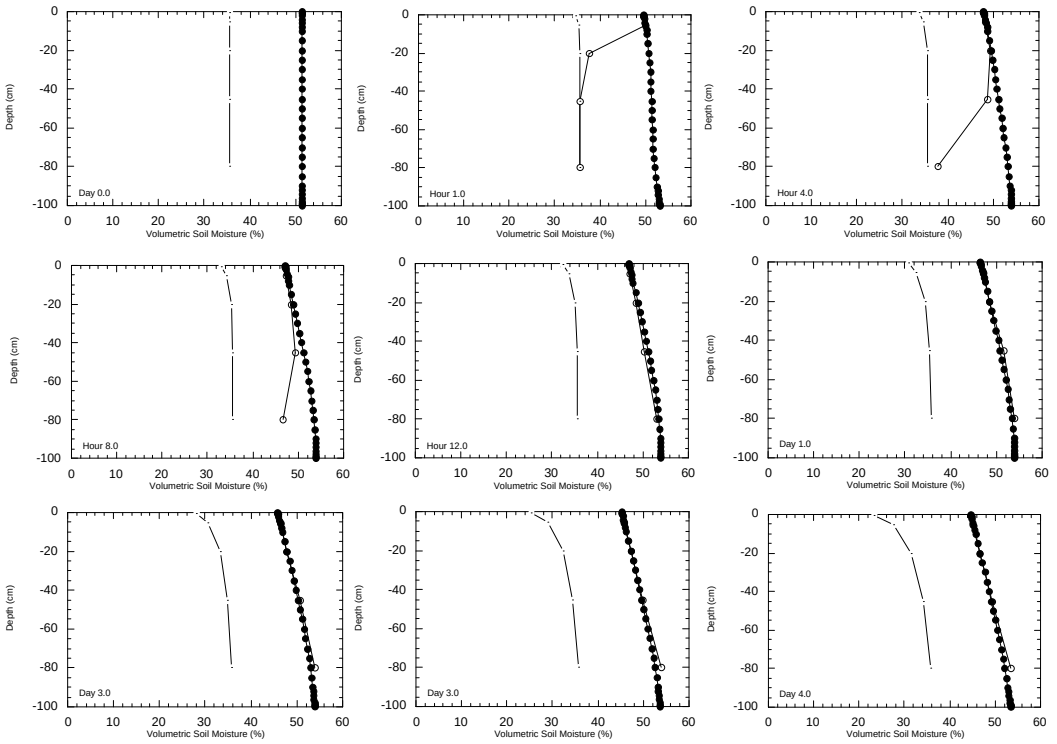

Figure 7.15: Comparison of soil moisture profile estimation using ABDOMEN1D with the version 3 distribution factor (open symbol), the open loop profile (open symbol with dot) and PROXSIM1D (closed symbol). The 5 layer model was updated once every hour using an observation depth of 1 cm layer; initial variances 0.25, system noise 5% of the state per hour and observation noise 2% of the state.

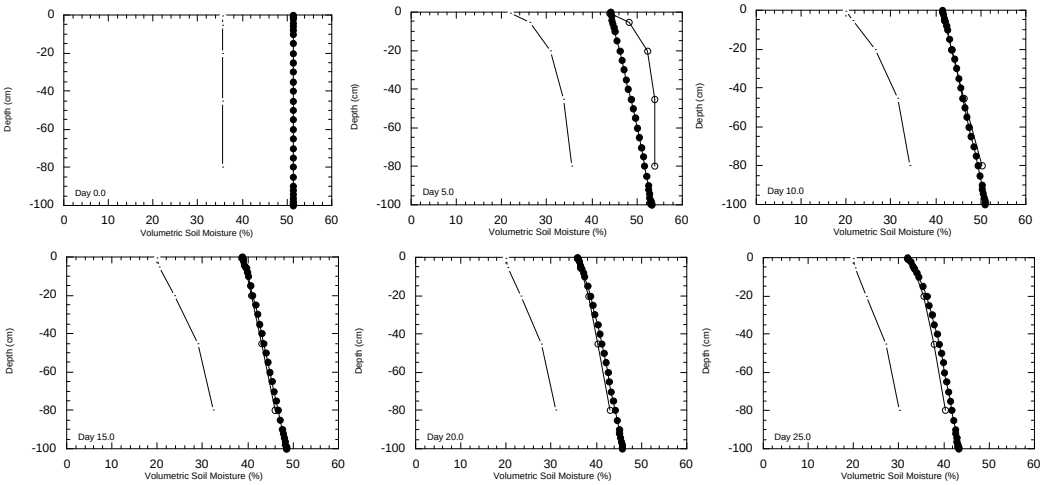

Figure 7.16: Comparison of soil moisture profile estimation using ABDOMEN1D with the version 3 distribution factor (open symbol), the open loop profile (open symbol with dot) and PROXSIM1D (closed symbol). The 5 layer model was updated once every 5 days using an observation depth of 1 cm layer; initial variances 0.25, system noise 5% of the state per hour and observation noise 2% of the state.

(i) the initial soil moisture profile is at field capacity θ_{fc}; (ii) the soil is of uniform depth D; (iii) the soil layer is underlain by an impermeable layer; (iv) the infiltration rate is greater than rainfall rate, such that there is no Hortonian overland flow; (v) that no sub-surface flow Q_{ss} occurs for soil moisture contents less than θ_{fc}; (vi) the rainfall has a uniform rate R; and (vii) the rainfall duration t_d extends beyond the time taken to obtain steady state t_s.

The equations describing sub-surface flow by this analytical solution to the kinematic equations are

$$Q_{ss} = \frac{K_s \cdot R \cdot t \cdot SLOPE}{\phi_e} \qquad 0 \le t < t_s;\ t_d > t_s \qquad (7.17a)$$

$$Q_{ss} = K_s \cdot D \cdot SLOPE \qquad t_s \le t \le t_r;\ t_d > t_s \qquad (7.17b)$$

$$Q_{ss} = R\left[L - (t - t_r)\frac{K_s \cdot SLOPE}{\phi_e} \right] \qquad t > t_r;\ t_d > t_s \qquad (7.17c),$$

where

$$t_s = \frac{\phi_e \cdot D}{R} \qquad (7.18a)$$

$$t_r = t_d + \frac{\phi_e}{K_s \cdot SLOPE}\left(L - \frac{K_s \cdot D \cdot SLOPE}{R} \right) \qquad (7.18b),$$

and K_S is the saturated hydraulic conductivity, t is the time since commencement of the rainfall event, $SLOPE$ is the hillslope gradient, L is the hillslope length, ϕ_e is the soil effective porosity given by $\phi_e = \phi - \theta_{fc}$, and t_r is the time at the commencement of the recession limb of the discharge hydrograph.

In comparing ABDOMEN3D with the analytical solution for a planar hillslope, the data given by Perera (1998) for a 12 m long and 1 m wide uniform

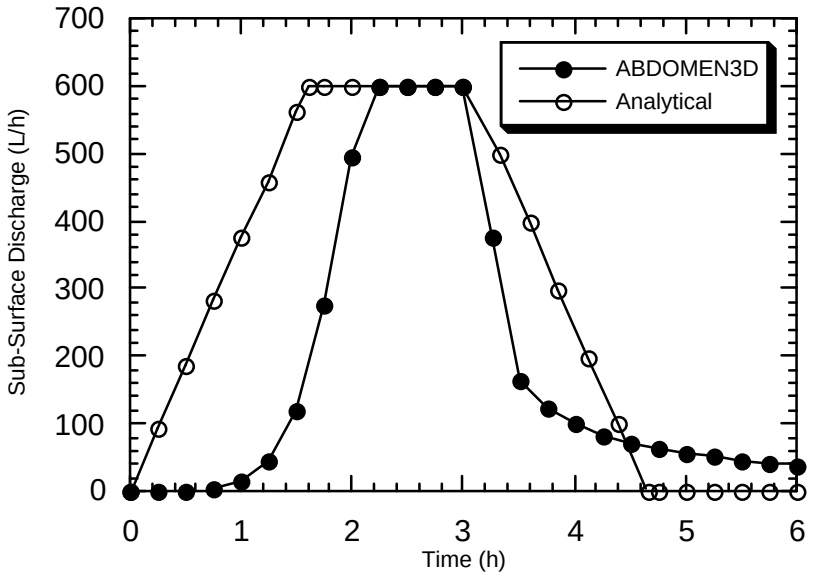

Figure 7.17: Comparison of sub-surface discharge hydrograph from ABDOMEN3D and an analytical solution to the kinematic wave equation for a planar catchment.

hillslope was applied. Soil within the hillslope was assumed to have an effective porosity of 0.04 and a saturated hydraulic conductivity of 1500 mm h^{-1}, to ensure that the infiltration rate exceeded the rainfall rate. The soil was 2 m deep and the catchment had a uniform slope of 0.2. A constant rainfall intensity of 50 mm h^{-1} was applied for 3 hours to ensure that steady state conditions were achieved.

As soil moisture is mobilised for soil moisture contents greater than the residual soil moisture content (when using the van Genuchten hydraulic conductivity relationship), the soil parameters used by ABDOMEN3D were an initial soil moisture content equal to the residual soil moisture content, having a value of 0, and hence a total porosity of 0.04. In this way, both models had the same amount of available storage, and mobilised sub-surface flow at the commencement of rainfall. However, the analytical solution uses the saturated hydraulic conductivity while ABDOMEN3D has a moisture dependent hydraulic conductivity. Thus, the ABDOMEN3D hydraulic conductivity was low until the soil moisture approached saturation.

Figure 7.17 shows a comparison between the sub-surface runoff from the analytical solution and the simplified catchment model ABDOMEN3D. This plot

shows the effect of assuming that hydraulic conductivity is at saturated hydraulic conductivity in the kinematic wave equation.

For the analytical solution, the rising limb of the hydrograph had a uniform gradient until steady state conditions were achieved. In contrast, ABDOMEN3D produced a rising limb that increased slowly at first, then as soil moisture content and hence hydraulic conductivity increased, the rising limb increased rapidly towards a uniform gradient, which was steeper than that for the analytical solution. The rising limb reached steady state with a delay of approximately 40 minutes after the analytical solution. Both solutions continued to discharge at steady state until the rainfall ceased, at which time both solutions commenced the recession limb (an artefact of the catchment configuration).

For the recession limb, the analytical solution again had a linear relationship for the discharge rate, while the discharge rate from ABDOMEN3D decreased as a function of soil moisture content and hydraulic conductivity. The gradient of sub-surface discharge from ABDOMEN3D was greater than that for the analytical solution for high soil moisture content, but progresses towards a low discharge rate as soil moisture content approached the initial soil moisture content.

7.5 CHAPTER SUMMARY

In this chapter, a computationally efficient soil moisture model has been developed, based on a conceptualisation of the Buckingham-Darcy moisture flux equation. This model has been shown to be an excellent approximation to the Richards equation, even when using only a few soil layers. Comparison with an analytical solution to the kinematic wave equation for sub-surface flow from a planar catchment yielded an adequate comparison, considering the approximations made by the kinematic wave equation.

Application of the soil moisture profile model ABDOMEN1D to the synthetic study presented in Chapter 5 showed that the θ-based soil moisture model yielded stable updates of the soil moisture profile for all simulations and update intervals tested. Furthermore, the simulation times required to retrieve the "true" soil moisture profile were comparable with the soil moisture transformed

version of the ψ-based Richards equation model in Chapter 6, but without the difficulties associated with transformation of the forecast system state covariance matrix into volumetric soil moisture space.

Simulation results with synthetic data have also shown that estimation of the "true" soil moisture profile with the Kalman-filter assimilation scheme is dependent on the model representation of the dominant soil physical processes. When the soil moisture model over-predicts or under-predicts the soil moisture profile storage for a given near-surface soil moisture content, then the soil moisture profile estimation is likely to be poor.